Quantitative relationship between in-plane and out-of-plane photonic spin Hall effects in vortex beams

Linguo Xie [1,*] Qingsong Liu [1] Hu Dou,[1] Zhaoxue Li,[2] and Xinxing Zhou [3,†]

[1]*Key Laboratory of Photonic and Optical Detection in Civil Aviation and Atmospheric Lidar Institute, Civil Aviation Flight University of China, Guanghan 618300, China*

[2]*Xinjiang Key Laboratory for Luminescence Minerals and Optical Functional Materials, School of Physics and Electronic Engineering, Xinjiang Normal University, Urumqi, Xinjiang 830054, China*

[3]*Key Laboratory of Low-Dimensional Quantum Structures and Quantum Control of Ministry of Education, School of Physics and Electronics, Hunan Normal University, Changsha 410081, China*

(Received 16 March 2025; revised 4 June 2025; accepted 15 July 2025; published 1 August 2025)

Over the years, the in-plane and out-of-plane photonic spin Hall effects (PSHEs) have been treated as two independent phenomena. In this work, we establish a unified framework that reveals the interrelationship between the in-plane and out-of-plane PSHEs for arbitrarily polarized vortex beams undergoing reflection and transmission. We quantitatively demonstrate how the vortex-induced in-plane spin spatial shift relates to the out-of-plane spin angular shift of the fundamental Gaussian beam (FGB). Similarly, we show that the vortex-dependent out-of-plane spin spatial shift is quantitatively connected to the in-plane spin angular shift of the FGB. Moreover, we find that the vortex-related in-plane and out-of-plane spin angular shifts remain unaffected by the FGB's in-plane and out-of-plane spin spatial shifts. Additionally, we confirm that all of our theoretical results adhere to the principles of linear and angular momentum conservation.

DOI: 10.1103/k3vg-pgpd

I. INTRODUCTION

Light reflection and transmission at an interface between two homogeneous isotropic media are fundamental optical processes described by Snell's law and Fresnel formulas, which define the geometrical-optics picture of light evolution [1]. Nevertheless, when dealing with finite-width optical beams, deviations from geometrical optics emerge at the wavelength scale, giving rise to the spatial and angular Goos–Hänchen (GH) and Imbert–Fedorov (IF) shifts [2–5]. These shifts appear as positional and directional variations, occurring both within and perpendicular to the plane of incidence, in the reflected and transmitted beams.

The photonic spin Hall effect (PSHE) [6–10], as an extension of the spatial IF shift, states that when a linearly polarized bounded beam undergoes reflection or refraction at an interface, its left-handed circular polarization (LCP) and right-handed circular polarization (RCP) components experience opposite shifts in the direction perpendicular to the plane of incidence. This phenomenon, also known as the out-of-plane PSHE, shares the same physical mechanism as the spatial IF shift, both originating from the interaction between the spin angular momentum (SAM) of light and extrinsic orbital angular momentum (OAM). Correspondingly, the LCP and RCP components can also experience opposite shifts in the direction parallel to the plane of incidence, a phenomenon referred to as the in-plane PSHE [11,12]. It is worth noting that the physical mechanism of the in-plane PSHE aligns with that of the angular GH shift, as both arise from the dispersion of Fresnel coefficients [13]. To date, out-of-plane and in-plane PSHEs have been extensively studied in various physical systems, including plasmonic structures [14–17], metamaterials [18–20], image edge detection [21,22], two-dimensional materials [23–26], the bound state in the continuum [27–29], and vortex beams [30,31].

Vortex beams, a kind of structured beams, possess intrinsic OAM and feature helical wave fronts [32,33]. In 2009, Bliokh *et al.* demonstrated a quantitative relationship between the vortex-dependent spatial IF shift and the angular GH shift of fundamental Gaussian beams (FGBs), as well as a similar quantitative relationship between the vortex-induced spatial GH shift and the angular IF shift of FGBs [34]. Given that the spatial IF shift shares the same physical mechanism as the out-of-plane PSHE and the angular GH shift shares the same mechanism as the in-plane PSHE, does a quantitative relationship also exist between the out-of-plane and in-plane PSHEs in vortex beams?

In this paper, we theoretically present explicit analytical expressions for the in-plane and out-of-plane PSHEs in the general case of arbitrarily polarized vortex beams and elaborate on their connections with linear and angular momentum conservation. Our analysis shows that the in-plane spin spatial shift of the vortex beam exhibits a quantitative relationship with the out-of-plane spin angular shift of the FGB. Similarly, the out-of-plane spin spatial shift of the vortex beam is quantitatively related to the in-plane spin angular shift of the FGB.

*Contact author: xielinguo05@163.com
†Contact author: xinxingzhou@hunnu.edu.cn

Published by the American Physical Society under the terms of the Creative Commons Attribution 4.0 International license. Further distribution of this work must maintain attribution to the author(s) and the published article's title, journal citation, and DOI.

Our study extends the work of Bliokh *et al.*, generalizing the spatial and angular GH and IF shifts of polarized vortex beams to encompass both in-plane and out-of-plane spin spatial and angular shifts.

II. THEORETICAL MODEL

A. Energy of LCP and RCP components

To simplify matters, we first consider the Fresnel reflection and transmission of the central plane wave in the beam. We assume that the polarization state of the incident central plane wave is arbitrary, which can be defined as

$$|\psi_i\rangle = C_p[(1+\alpha_c)|+\rangle + (1-\alpha_c)|-\rangle], \tag{1}$$

where $C_p = 1/\sqrt{2(1+|\alpha_c|^2)}$ is the normalization constant related to the polarization state, and $1+\alpha_c$ and $1-\alpha_c$ are polarization components of the Jones vector on the basis of the LCP state $|+\rangle$ and the RCP state $|-\rangle$. It is worth noting that α_c is a complex number. A value of $\alpha_c = 1$ indicates an LCP state, while a value of $\alpha_c = -1$ represents an RCP state. $\alpha_c = 0$ and $\alpha_c = -\infty i$ correspond to the horizontal and vertical linear polarizations, respectively. Upon partial reflection and transmission at an interface between two homogeneous isotropic media, the polarization states of the secondary beams are determined by applying the Fresnel–Jones matrix $\hat{F}_b$,

$$|\psi_b\rangle = \hat{F}_b|\psi_i\rangle, \quad \hat{F}_b = \begin{bmatrix} b_{++} & b_{+-} \\ b_{-+} & b_{--} \end{bmatrix}, \tag{2}$$

where $b = r, t$ corresponds to the beam's reflection and transmission, respectively. Note that $b_{++} = b_{--} = (b_p + b_s)/2$ and $b_{+-} = b_{-+} = (b_p - b_s)/2$ are Fresnel coefficients on the basis of circular polarization. b_{++} and b_{--} represent polarization-preserving amplitude components (LCP $\rightarrow$ LCP, RCP $\rightarrow$ RCP), whereas b_{+-} and b_{-+} represent polarization-converting components (RCP $\rightarrow$ LCP, LCP $\rightarrow$ RCP). b_p and b_s are Fresnel coefficients on the basis of TM (p) and TE (s) modes with respect to the interface.

Based on the above analysis, the polarization states of the secondary beams can be expressed as $|\psi_b\rangle = C_p(|\psi_{b+}\rangle + |\psi_{b-}\rangle)$, where $|\psi_{b+}\rangle = b_{++}(1+\alpha_c)|+\rangle + b_{+-}(1-\alpha_c)|+\rangle$ and $|\psi_{b-}\rangle = b_{-+}(1+\alpha_c)|-\rangle + b_{--}(1-\alpha_c)|-\rangle$ represent the LCP and RCP components of the secondary beams, respectively. The normalized polarization states $|e_b\rangle$ for the central plane wave take the form

$$|e_b\rangle = Q_b^{-1}|\psi_b\rangle, \quad Q_b^2 = \langle\psi_b|\psi_b\rangle = C_p^2\left(Q_{b+}^2 + Q_{b-}^2\right). \tag{3}$$

Here, $Q_{b+}^2 = \langle\psi_{b+}|\psi_{b+}\rangle$ and $Q_{b-}^2 = \langle\psi_{b-}|\psi_{b-}\rangle$. Q_b represent the amplitude coefficients of the fields, while their energy coefficients, which satisfy the conservation law, are expressed as follows:

$$\sum_{b=r,t}(\mathsf{Q}_{b+} + \mathsf{Q}_{b-}) = 1. \tag{4}$$

Here, $\mathsf{Q}_{b+} = n_b|\gamma_b|C_p^2Q_{b+}^2$ and $\mathsf{Q}_{b-} = n_b|\gamma_b|C_p^2Q_{b-}^2$ represent the normalized energy coefficients of the LCP and RCP components of the secondary beams, respectively. n_b is the relative refractive index of the medium, i.e., $n_r = n_i = 1$ and $n_t = n$. $\gamma_b = \cos\theta_b/\cos\theta_i$, i.e., $\gamma_r = \cos\theta_r/\cos\theta_i = -1$ and $\gamma_t = \cos\theta_t/\cos\theta_i$. θ_i, θ_r, and θ_t denote the angles of incidence, reflection, and transmission, respectively. Note that we use $\theta_r = \pi - \theta_i$ and $\theta_t = \sin^{-1}(n^{-1}\sin\theta_i)$.

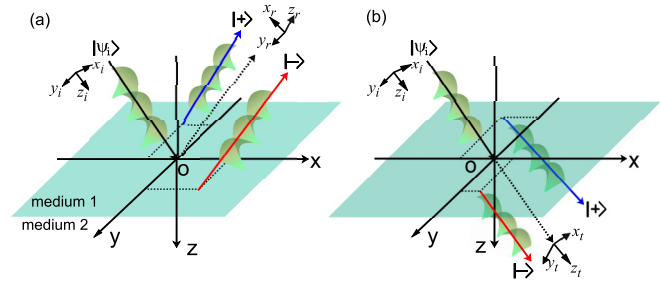


FIG. 1. Schematic diagram of the vortex beam reflection (a) and transmission (b).

B. In-plane and out-of-plane spin spatial and angular shifts

Next, we employ the angular spectrum method to develop a model describing the partial reflection and transmission of vortex beams at the interface between two homogeneous isotropic media, as illustrated in Figs. 1(a) and 1(b). We define the laboratory Cartesian coordinate system as (x, y, z) and the local coordinate system as (x_a, y_a, z_a), where y and y_a are aligned in the same direction (see Fig. 1). The subscript $a = i, r, t$ corresponds to the beam's incidence, reflection, and transmission, respectively.

We consider the incident beam as arbitrarily polarized, and its wave function can be written as follows:

$$|\Psi_i\rangle = \iint dk_{x_i}dk_{y_i}\Phi(k_{x_i}, k_{y_i})\left|k_{x_i}\right\rangle\left|k_{y_i}\right\rangle|\psi_i\rangle. \tag{5}$$

$\Phi(k_{x_i}, k_{y_i})$ is the angular spectrum distribution function of the beam, which determines the contribution of each plane-wave component to the overall beam. $|k_{x_i}\rangle|k_{y_i}\rangle$ is a direct product of wave-vector eigenstates, representing a plane-wave eigenstate with transverse wave-vector components k_{x_i} and k_{y_i} along the x_i and y_i directions, respectively.

For the incident vortex beams, $\iint dk_{x_i}dk_{y_i}\Phi(k_{x_i}, k_{y_i})|k_{x_i}\rangle|k_{y_i}\rangle = \frac{C_l\omega_0}{2}[\frac{\omega_0(-ik_{x_i}+\mathrm{sgn}[l]k_{y_i})}{\sqrt{2}}]^{|l|}\exp[-\frac{(\omega_0k_{x_i})^2+(\omega_0k_{y_i})^2}{4}]$. Here, l is the topological charge, $C_l = \sqrt{2/(\pi|l|!)}$ is the normalization constant, ω_0 is the beam waist, and $\mathrm{sgn}[l]$ is the sign function. Due to the in-plane deflection changing the angle of incidence and the out-of-plane deflection altering the plane of incidence about the z axis, the Fresnel–Jones matrix that connects the incident and secondary fields in the beam coordinate frames needs to be modified [5,35]. By applying the boundary conditions $k_{y_b} = k_{y_i}$ and $k_{x_b} = k_{x_i}/\gamma_b$, the corrected relationship between the incident and secondary fields can be represented using the modified Fresnel–Jones matrix $\hat{Y}_b$:

$$|\Psi_b\rangle = \hat{Y}_b|\Psi_i\rangle, \quad \hat{Y}_b = \begin{bmatrix} b_{++(\theta_i)}\exp\left(k_{x_b}\Delta_{x_{b++}}\right)\exp\left(-ik_{y_b}\delta_{y_{b++}}\right) & b_{+-(\theta_i)}\exp\left(k_{x_b}\Delta_{x_{b+-}}\right)\exp\left(-ik_{y_b}\delta_{y_{b+-}}\right) \\ b_{-+(\theta_i)}\exp\left(k_{x_b}\Delta_{x_{b-+}}\right)\exp\left(-ik_{y_b}\delta_{y_{b-+}}\right) & b_{--(\theta_i)}\exp\left(k_{x_b}\Delta_{x_{b--}}\right)\exp\left(-ik_{y_b}\delta_{y_{b--}}\right) \end{bmatrix}. \tag{6}$$

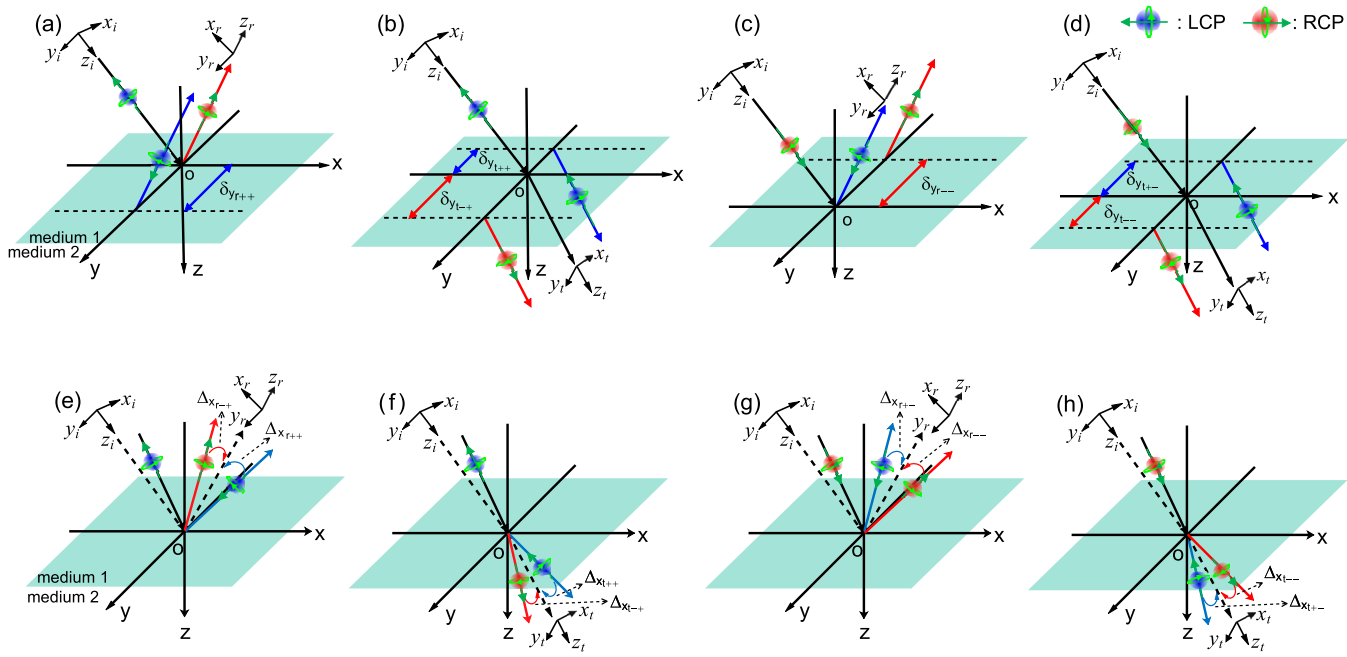


FIG. 2. (a) and (b) represent the out-of-plane spin spatial shifts of the LCP and RCP components during reflection and transmission for an incident LCP beam, while (c) and (d) correspond to those shifts for an incident RCP beam. Similarly, (e) and (f) denote the in-plane spin angular shifts of the LCP and RCP components for an incident LCP beam, whereas (g) and (h) show the corresponding shifts for an incident RCP beam. In panels (e)–(h), the dashed lines represent the direction of the central wave vector. The blue and red circles represent LCP and RCP, respectively, and the green arrows indicate the direction of SAM. $\delta_{y_{r+-}} = \delta_{y_{r-+}} = 0$ is not shown in the figure.

Here, $b_{++(\theta_i)}$, $b_{+-(\theta_i)}$, $b_{-+(\theta_i)}$, and $b_{--(\theta_i)}$ are Fresnel coefficients corresponding to the central wave vector. $\delta_{y_{b++}} = \cot\theta_i\,(1 - \gamma_b)/k_0$, $\delta_{y_{b-+}} = \cot\theta_i(1+\gamma_b)/k_0$, $\delta_{y_{b+-}} = -\delta_{y_{b-+}}$, $\delta_{y_{b--}} = -\delta_{y_{b++}}$, $\Delta_{x_{b++}} = \gamma_b\,(\partial \ln b_{++}/\partial\,\theta_i)/k_0$, $\Delta_{x_{b-+}} = \gamma_b(\partial \ln b_{-+}/\partial\theta_i)/k_0$, $\Delta_{x_{b+-}} = \Delta_{x_{b-+}}$, and $\Delta_{x_{b--}} = \Delta_{x_{b++}}$. k_0 is the wave number in the first medium. $\delta_{y_{b++}}$ and $\delta_{y_{b-+}}$ represent the out-of-plane spin spatial shifts of the LCP and RCP components, respectively, for an incident LCP beam, while $\delta_{y_{b+-}}$ and $\delta_{y_{b--}}$ represent the corresponding shifts for an incident RCP beam [36,37]. $\Delta_{x_{b++}}$ and $\Delta_{x_{b-+}}$ denote the in-plane spin angular shifts of the LCP and RCP components for an incident LCP beam, whereas $\Delta_{x_{b+-}}$ and $\Delta_{x_{b--}}$ indicate the corresponding angular shifts for an incident RCP beam [11,37]. Their specific shifts are shown in Fig. 2. The physical mechanism for spin spatial shifts along the y direction arises from the spin-orbit coupling of one photon [7]. In contrast, the spin angular shifts in the x direction are due to the spatial dispersion characteristics of the Fresnel coefficients [37], which can also be interpreted as the first-order expansion of the Fresnel coefficients with respect to the in-plane wave vector.

Generally, the modified Fresnel–Jones matrix is expressed in the basis of linear polarization [5,35]. For the conversion from the linear polarization basis to the circular polarization basis, see Appendix A.

The paraxial wave equation can be formally identified with the two-dimensional Schrödinger equation, with the coordinate z taking the role of time t. This correspondence has established the operator approach introduced by Stoler as a particularly effective framework for addressing problems in physical optics [38–40]. In what follows, we leverage this operator formalism to determine the spin spatial and angular shifts of both reflected and transmitted beams. Therefore, for an arbitrary input polarization, the in-plane and out-of-plane spin spatial and angular shifts for the LCP and RCP components of the secondary field can be obtained with

$$\delta_{x_{b+}} = \frac{\langle\Psi_{b+}|i\frac{\partial}{\partial k_{x_b}}|\Psi_{b+}\rangle}{\langle\Psi_{b+}|\Psi_{b+}\rangle} = \delta_{x_{b+}}|_{l=0} + \frac{l\gamma_b R}{k_0}\big(\Delta_{y_{b+}}|_{l=0}\big), \quad (7a)$$

$$\delta_{x_{b-}} = \frac{\langle\Psi_{b-}|i\frac{\partial}{\partial k_{x_b}}|\Psi_{b-}\rangle}{\langle\Psi_{b-}|\Psi_{b-}\rangle} = \delta_{x_{b-}}|_{l=0} + \frac{l\gamma_b R}{k_0}\big(\Delta_{y_{b-}}|_{l=0}\big), \quad (7b)$$

$$\delta_{y_{b+}} = \frac{\langle\Psi_{b+}|i\frac{\partial}{\partial k_{y_b}}|\Psi_{b+}\rangle}{\langle\Psi_{b+}|\Psi_{b+}\rangle} = \delta_{y_{b+}}|_{l=0} - \frac{l\gamma_b R}{k_0}\big(\Delta_{x_{b+}}|_{l=0}\big), \quad (7c)$$

$$\delta_{y_{b-}} = \frac{\langle\Psi_{b-}|i\frac{\partial}{\partial k_{y_b}}|\Psi_{b-}\rangle}{\langle\Psi_{b-}|\Psi_{b-}\rangle} = \delta_{y_{b-}}|_{l=0} - \frac{l\gamma_b R}{k_0}\big(\Delta_{x_{b-}}|_{l=0}\big), \quad (7d)$$

$$\Delta_{x_{b+}} = \frac{\langle\Psi_{b+}|k_{x_b}|\Psi_{b+}\rangle}{\langle\Psi_{b+}|\Psi_{b+}\rangle} = (|l|+1)\big(\Delta_{x_{b+}}|_{l=0}\big), \quad (8a)$$

$$\Delta_{x_{b-}} = \frac{\langle\Psi_{b-}|k_{x_b}|\Psi_{b-}\rangle}{\langle\Psi_{b-}|\Psi_{b-}\rangle} = (|l|+1)\big(\Delta_{x_{b-}}|_{l=0}\big), \quad (8b)$$

$$\Delta_{y_{b+}} = \frac{\langle\Psi_{b+}|k_{y_b}|\Psi_{b+}\rangle}{\langle\Psi_{b+}|\Psi_{b+}\rangle} = (|l|+1)\big(\Delta_{y_{b+}}|_{l=0}\big), \quad (8c)$$

$$\Delta_{y_{b-}} = \frac{\langle\Psi_{b-}|k_{y_b}|\Psi_{b-}\rangle}{\langle\Psi_{b-}|\Psi_{b-}\rangle} = (|l|+1)\big(\Delta_{y_{b-}}|_{l=0}\big). \quad (8d)$$

Here,

$$\delta_{x_{b+}}|_{l=0} = -\frac{\Delta_{x_{b++}} \operatorname{Im}\eta_{b++} + \Delta_{x_{b+-}} \operatorname{Im}\eta_{b+-}}{Q_{b+}^2}, \tag{9a}$$

$$\delta_{x_{b-}}|_{l=0} = -\frac{\Delta_{x_{b-+}} \operatorname{Im}\eta_{b-+} + \Delta_{x_{b--}} \operatorname{Im}\eta_{b--}}{Q_{b-}^2}, \tag{9b}$$

$$\delta_{y_{b+}}|_{l=0} = \frac{\delta_{y_{b++}} \operatorname{Re}\eta_{b++} + \delta_{y_{b+-}} \operatorname{Re}\eta_{b+-}}{Q_{b+}^2}, \tag{9c}$$

$$\delta_{y_{b-}}|_{l=0} = \frac{\delta_{y_{b-+}} \operatorname{Re}\eta_{b-+} + \delta_{y_{b--}} \operatorname{Re}\eta_{b--}}{Q_{b-}^2}, \tag{9d}$$

$$\Delta_{x_{b+}}|_{l=0} = \frac{k_0\left(\Delta_{x_{b++}} \operatorname{Re}\eta_{b++} + \Delta_{x_{b+-}} \operatorname{Re}\eta_{b+-}\right)}{R\gamma_b^2 Q_{b+}^2}, \tag{10a}$$

$$\Delta_{x_{b-}}|_{l=0} = \frac{k_0\left(\Delta_{x_{b-+}} \operatorname{Re}\eta_{b-+} + \Delta_{x_{b--}} \operatorname{Re}\eta_{b--}\right)}{R\gamma_b^2 Q_{b-}^2}, \tag{10b}$$

$$\Delta_{y_{b+}}|_{l=0} = \frac{k_0\left(\delta_{y_{b++}} \operatorname{Im}\eta_{b++} + \delta_{y_{b+-}} \operatorname{Im}\eta_{b+-}\right)}{RQ_{b+}^2}, \tag{10c}$$

$$\Delta_{y_{b-}}|_{l=0} = \frac{k_0\left(\delta_{y_{b-+}} \operatorname{Im}\eta_{b-+} + \delta_{y_{b--}} \operatorname{Im}\eta_{b--}\right)}{RQ_{b-}^2}. \tag{10d}$$

Note that δ and Δ represent the spatial and angular shifts, x and y represent the in-plane and out-of-plane directions, $+$ and $-$ correspond to the LCP and RCP components, Im and Re denote the imaginary and real parts, and $|\Psi_{b+}\rangle$ and $|\Psi_{b-}\rangle$ are the wave functions of the LCP and RCP components of the secondary field, with detailed expressions provided in Appendix B. $l = 0$ corresponds to the FGB. $R = k_0\omega_0^2/2$ is the Rayleigh length. η_{b++}, η_{b+-}, η_{b-+}, and η_{b--} are the complex weighting coefficients, with their specific expressions given as follows:

$$\eta_{b++} = \langle +|b_{++}(1+\alpha_c^*)|\psi_{b+}\rangle, \tag{11a}$$

$$\eta_{b+-} = \langle +|b_{+-}(1-\alpha_c^*)|\psi_{b+}\rangle, \tag{11b}$$

$$\eta_{b-+} = \langle -|b_{-+}(1+\alpha_c^*)|\psi_{b-}\rangle, \tag{11c}$$

$$\eta_{b--} = \langle -|b_{--}(1-\alpha_c^*)|\psi_{b-}\rangle. \tag{11d}$$

Here, α_c^* is the complex conjugate of α_c. All Fresnel coefficients are real numbers, as our analysis is limited to partial reflection and transmission at an interface between two homogeneous isotropic media. For isotropic complex interfaces (e.g., the air–nanometal film interface and the air–monolayer graphene interface) and total internal reflection, we can replace the real Fresnel coefficients with complex Fresnel coefficients. However, for anisotropic complex interfaces (e.g., metasurfaces and topological insulators), we must take into account the tensorial permittivity and permeability, incorporate the boundary conditions, and revise the derivation of the Fresnel reflection and transmission coefficients. Then, by following a derivation process similar to that in Appendix A, we can obtain the corrected Fresnel–Jones matrix tailored for anisotropic complex interfaces.

It is well known that the arbitrary incident polarization state can be decomposed into a linear combination of LCP and RCP states; see Eq. (1). Here, η_{b++} (η_{b-+}) and η_{b+-} (η_{b--}) represent the weighting coefficients for the conversion of the incident LCP and RCP components into the LCP (RCP) component of the secondary field, respectively. It is important to note that all of these weighting coefficients are complex valued. The real components correspond to the conversion of spatial shifts to spatial shifts and angular shifts to angular shifts [see Eqs. (9c), (9d), (10a), and (10b)], whereas the imaginary components correspond to the conversion of angular shifts to spatial shifts and spatial shifts to angular shifts [see Eqs. (9a), (9b), (10c), and (10d)].

Equations (9a)–(9d) and (10a)–(10d) demonstrate that, for an FGB with arbitrary input polarization, the spin shifts—both in-plane and out-of-plane, spatial and angular, LCP and RCP, reflected and transmitted—share the same structural expression. Consequently, our work establishes a unified framework that highlights the high degree of symmetry among the various spin shifts of the beam.

Equations (7a)–(7d) and (8a)–(8d) are the main results of this paper. They succinctly reveal the quantitative relationship between the in-plane and out-of-plane PSHEs in the most general case of an arbitrarily polarized vortex beam.

From Eq. (7a), we observe that the in-plane spin spatial shift of the vortex beam can be expressed as a linear combination of the in-plane spin spatial shift and the out-of-plane spin angular shift of the FGB. This linear relationship indicates that the in-plane spin shift of the vortex beam results from the combined effect of two shift terms: $\delta_{x_{b+}}|_{l=0}$, which is unrelated to the intrinsic OAM, and $l\gamma_b R(\Delta_{y_{b+}}|_{l=0})/k_0$, which is related to it.

The shift term $\delta_{x_{b+}}|_{l=0}$ indicates that the presence of intrinsic OAM does not directly affect the in-plane spin spatial shift induced by the dispersion of the Fresnel coefficients. However, the shift term $l\gamma_b R(\Delta_{y_{b+}}|_{l=0})/k_0$ involves two sequential processes. The first is the generation of an out-of-plane spin angular shift $\Delta_{y_{b+}}|_{l=0}$, which arises from the coupling between the SAM and the external OAM. This angular shift then couples with the intrinsic OAM, ultimately giving rise to the shift term $l\gamma_b R(\Delta_{y_{b+}}|_{l=0})/k_0$ associated with the intrinsic OAM. These conclusions also apply to Eq. (7b).

Likewise, Eq. (7c) reveals that the out-of-plane spin spatial shift of the vortex beam arises from a linear combination of the out-of-plane spin spatial shift and the in-plane spin angular shift of the FGB. This linear relationship indicates that the out-of-plane spin shift of the vortex beam results from the combined effect of two shift terms: $\delta_{y_{b+}}|_{l=0}$, which is unrelated to the intrinsic OAM, and $-l\gamma_b R(\Delta_{x_{b+}}|_{l=0})/k_0$, which is related to it.

The shift term $\delta_{y_{b+}}|_{l=0}$ indicates that the presence of intrinsic OAM does not directly affect the out-of-plane spin spatial shift induced by the coupling between the SAM and the external OAM. However, the shift term $-l\gamma_b R(\Delta_{x_{b+}}|_{l=0})/k_0$ also involves two sequential processes. The first is the generation of an in-plane spin angular shift $\Delta_{x_{b+}}|_{l=0}$, which arises from the dispersion of the Fresnel coefficients. This angular shift then couples with the intrinsic OAM, ultimately giving rise to the shift term $-l\gamma_b R(\Delta_{x_{b+}}|_{l=0})/k_0$ associated with the intrinsic OAM. These conclusions also apply to Eq. (7d).

However, Eqs. (8a)–(8d) indicate that the in-plane and out-of-plane spin angular shifts of the vortex beam are independent of the spin spatial shifts of the FGB and depend solely on the spin angular shifts of the FGB. Equations (8a)–(8d) show that the spin angular shift of the vortex beam amplifies

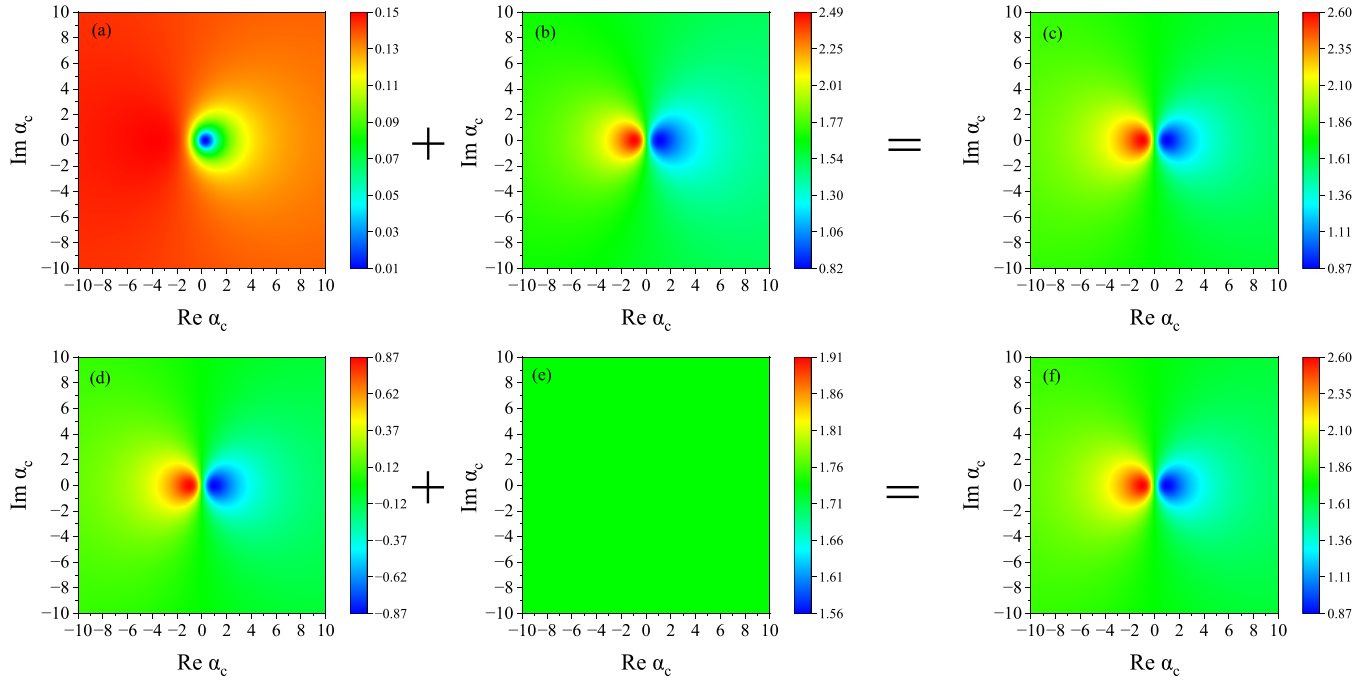


FIG. 3. (a) and (b) respectively illustrate the variation of the z component of the total angular momentum of the reflected and transmitted beams with the incident polarization state. (c) represents the sum of (a) and (b). (d) and (e) respectively show the variation of the z component of the SAM and OAM of the incident beam with the incident polarization state. (f) is the sum of (d) and (e). The parameters are incident angle $\theta_i = \pi/6$, refractive index of the transmitting medium $n = 1.5$, topological charge $l = 2$, wavelength $\lambda = 632.8$ nm, and beam waist $\omega_0 = 27$ μm.

the spin angular shift of the FGB by a factor of $|l| + 1$. Our work extends the study of Bliokh *et al.* to spin-dependent scenarios [34].

Moreover, based on the boundary condition $k_{x_t} = k_{x_i}/\gamma_t$, the cross-sectional geometry of the beam transitions from a circular profile to an elliptical profile during transmission, resulting in two types of geometry-related shifts that are independent of polarization. One type is an additional spatial shift along the y_t direction, while the other is an additional angular shift along the x_t direction. The y_t-directional additional spatial shift arises from the difference in the z components of intrinsic OAM at the transmission and can be expressed as $\delta_{y_t}^{add} = \frac{l}{2k_0}\cot\theta_i(\gamma_t^2 - 1)$ [34]. The x_t-directional additional angular shift stems from the first-order derivative of γ_t with respect to the in-plane wave vector in its Taylor expansion and can be written as $\Delta_{x_t}^{add} = (|l| + 1)\frac{1}{2R\gamma_t^2}\frac{\partial\gamma_t}{\partial\theta_i}$. This angular shift has not been reported in other studies, and a detailed derivation is provided in Appendix C. Finally, the corrected expressions for the in-plane and out-of-plane spin spatial and angular shifts can be written as

$$\langle x_{b+}\rangle = \delta_{x_{b+}}, \tag{12a}$$
$$\langle x_{b-}\rangle = \delta_{x_{b-}}, \tag{12b}$$
$$\langle y_{b+}\rangle = \delta_{y_{b+}} + \delta_{y_b}^{add}, \tag{12c}$$
$$\langle y_{b-}\rangle = \delta_{y_{b-}} + \delta_{y_b}^{add}, \tag{12d}$$
$$\langle k_{x_{b+}}\rangle = \Delta_{x_{b+}} + \Delta_{x_b}^{add}, \tag{13a}$$
$$\langle k_{x_{b-}}\rangle = \Delta_{x_{b-}} + \Delta_{x_b}^{add}, \tag{13b}$$
$$\langle k_{y_{b+}}\rangle = \Delta_{y_{b+}}, \tag{13c}$$
$$\langle k_{y_{b-}}\rangle = \Delta_{y_{b-}}. \tag{13d}$$

Here, $\delta_{y_b}^{add} = \frac{l}{2k_0}\cot\theta_i(\gamma_b^2 - 1)$ and $\Delta_{x_b}^{add} = (|l| + 1)\frac{1}{2R\gamma_b^2}\frac{\partial\gamma_b}{\partial\theta_i}$. For the reflection process, let $b = r$, with $\gamma_r = -1$, resulting in $\delta_{y_r}^{add} = 0$ and $\Delta_{x_r}^{add} = 0$. $\langle x_{b+}\rangle$ and $\langle x_{b-}\rangle$ represent the total in-plane spin spatial shifts, $\langle y_{b+}\rangle$ and $\langle y_{b-}\rangle$ the total out-of-plane spin spatial shifts, $\langle k_{x_{b+}}\rangle$ and $\langle k_{x_{b-}}\rangle$ the total in-plane spin angular shifts, and $\langle k_{y_{b+}}\rangle$ and $\langle k_{y_{b-}}\rangle$ the total out-of-plane spin angular shifts for the LCP and RCP.

III. LINEAR AND ANGULAR MOMENTUM CONSERVATION

It can be verified that the spin angular shifts adhere to a constraint derived from the conservation of linear momentum. The balance of the tangential components of the beam's momentum leads to the following equations:

$$\sum_{b=r,t}\left(\mathrm{Q}_{b+}\langle k_{x_{b+}}\rangle + \mathrm{Q}_{b-}\langle k_{x_{b-}}\rangle\right)\cos\theta_b = 0, \tag{14a}$$
$$\sum_{b=r,t}\left(\mathrm{Q}_{b+}\langle k_{y_{b+}}\rangle + \mathrm{Q}_{b-}\langle k_{y_{b-}}\rangle\right) = 0. \tag{14b}$$

Equations (14a) and (14b) show the spin angular shifts fulfill conservation laws for the x and y components of total linear momentum. We employ the momentum transformation relation in the x-direction between the laboratory Cartesian coordinate system and the local coordinate system, together with Snell's law. Note that we use $\hbar = 1$. Substituting Eqs. (11a)–(11d) into (10a)–(10d), and using relations (8a)–(8d) and (13a)–(13d), it can be proven that the spin angular shifts fulfill Eqs. (14a) and (14b) identically.

Notably, the spin spatial shift is closely associated with the conservation of the spin-orbit angular momentum of light. Moreover, the rotational symmetry of the medium around the z axis ensures that the z component of the total angular momentum is conserved during reflection and transmission. The conservation of the z component of the total angular momentum in the scattering can be written as

$$\sum_{b=r,t}\left[\mathsf{Q}_{b+}\left(\langle S_{z_{b+}}\rangle+\langle L^{int}_{z_{b+}}\rangle+\langle L^{out}_{z_{b+}}\rangle\right)+\mathsf{Q}_{b-}\left(\langle S_{z_{b-}}\rangle\right.\right.$$
$$\left.\left.+\langle L^{int}_{z_{b-}}\rangle+\langle L^{out}_{z_{b-}}\rangle\right)\right]=\langle S_{z_i}\rangle+\langle L^{int}_{z_i}\rangle. \tag{15}$$

Here, based on the definition of SAM and OAM [5,41], $\langle S_{z_{b+}}\rangle=-\cos\theta_b$ and $\langle S_{z_{b-}}\rangle=\cos\theta_b$ represent the z components of the SAM of the LCP and RCP components of the secondary beams, respectively. $\langle L^{int}_{z_{b+}}\rangle=\frac{1}{2}(\gamma_b+\frac{1}{\gamma_b})l\cos\theta_b$ and $\langle L^{int}_{z_{b-}}\rangle=\frac{1}{2}(\gamma_b+\frac{1}{\gamma_b})l\cos\theta_b$ represent the z components of the intrinsic OAM (vortex) of the LCP and RCP components of the secondary beams. Noting that $\langle L^{int}_{z_{b+}}\rangle=\langle L^{int}_{z_{b-}}\rangle$ indicates that spin has no effect on the intrinsic OAM, meaning there is no interaction between the SAM and the intrinsic OAM. $\langle L^{out}_{z_{b+}}\rangle=-\langle y_{b+}\rangle k_b\sin\theta_b$ and $\langle L^{out}_{z_{b-}}\rangle=-\langle y_{b-}\rangle k_b\sin\theta_b$ represent the z components of the extrinsic OAM (trajectory) of the LCP and RCP components of the secondary beams. Here, k_b is the wave number of the secondary beams. $\langle S_{z_i}\rangle=-\langle S_i\rangle\cos\theta_i$ represents the z components of the SAM of incident beam, where $\langle S_i\rangle=\langle\psi_i|\hat{\sigma}_3|\psi_i\rangle=4C_p^2\,\mathrm{Re}\,\alpha_c$ is the helicity of incident beam and $\hat{\sigma}_3=\mathrm{diag}(1,-1)$ is the Pauli matrix[7]. $\langle L^{int}_{z_i}\rangle=l\cos\theta_i$ denotes the z component of the intrinsic OAM of the incident beam. Substituting Eqs. (11a)–(11d) into (9c), (9d), (10a), and (10b), and using relations (7c), (7d), (12c), and (12d), one can verify that Eq. (15) is fulfilled identically.

To visually demonstrate the validity of Eq. (15), we have plotted Fig. 3. As shown in Fig. 3, the sum of the z components of the total angular momentum of the reflected and transmitted beams [see Fig. 3(c)] equals the sum of the z components of the SAM and OAM of the incident beam [see Fig. 3(f)]. Note that, based on Eq. (1), it can be readily observed that $\mathrm{Re}\,\alpha_c$ and $\mathrm{Im}\,\alpha_c$ together determine the incident polarization state.

Finally, since our work is built on the foundational framework established by Bliokh *et al.* [34], there are certain similarities between the two studies. To highlight the distinctions and advancements introduced in our approach, we systematically summarize the key differences and present them in Appendix D.

IV. CONCLUSIONS

In conclusion, we have developed a unified theoretical framework and provided explicit analytical formulas describing the in-plane and out-of-plane PSHEs occurring when an arbitrarily polarized vortex beam is reflected and transmitted at an interface between two media. Our findings reveal that the in-plane spin spatial shift of the vortex beam exhibits a quantitative relationship with the out-of-plane spin angular shift of the FGB, and, conversely, the out-of-plane spin spatial shift of the vortex beam is quantitatively related to the in-plane spin angular shift of the FGB. All theoretical results are verified to be consistent with the conservation of linear and angular momentum. Given that our results are solely based on the spin-orbit coupling of one photon, as well as the spatial dispersion characteristics of the Fresnel coefficients and their dependence on spin energy, we anticipate that this work may provide insights for addressing the in-plane and out-of-plane photonic spin spatial and angular shifts of arbitrarily structured paraxial beams.

ACKNOWLEDGMENTS

This paper was supported by the National Natural Science Foundation of China (Grants No. 12404374, No. 12464058, No. 12374273, No. 12421005, No. 42406184, and No. 62341507) and the Hunan Provincial Major Sci-Tech Program (Grant No. 2023ZJ1010).

DATA AVAILABILITY

The data that support the findings of this article are not publicly available upon publication because it is not technically feasible and/or the cost of preparing, depositing, and hosting the data would be prohibitive within the terms of this research project. The data are available from the authors upon reasonable request.

APPENDIX A: MODIFIED FRESNEL–JONES MATRIX FROM THE LINEAR POLARIZATION BASIS TO THE CIRCULAR POLARIZATION BASIS

First, for the central plane wave, the Jones matrix relating the incident and secondary fields in the beam coordinate frames can be expressed as

$$\hat{U}_b=\begin{bmatrix}b_p & 0\\ 0 & b_s\end{bmatrix}, \tag{A1}$$

where $b=r,t$ corresponds to the beam's reflection and transmission, respectively. b_p and b_s are Fresnel coefficients on the basis of TM (p) and TE (s) modes with respect to the interface.

Second, for the vortex beam, due to the out-of-plane deflection altering the plane of incidence about the z axis [5,35], the modified Jones matrix relating the incident and secondary fields in the beam coordinate frames can be expressed as

$$\hat{V}_b=\begin{bmatrix}b_p & \frac{k_{y_b}(b_p-\gamma_b b_s)\cot\theta_i}{k_0}\\ -\frac{k_{y_b}(b_s-\gamma_b b_p)\cot\theta_i}{k_0} & b_s\end{bmatrix}, \tag{A2}$$

where k_{y_b} is the wave-vector component along the y_b axe. k_0 is the wave number in the first medium (air). θ_i is the incident angle. For reflection process, $\gamma_b=\gamma_r=-1$; for transmission process, $\gamma_b=\gamma_t=\cos\theta_t/\cos\theta_i$.

Then, for the vortex beam, due to the in-plane deflection changing the angle of incidence [5], we need to consider the spatial dispersion characteristics of the Fresnel coefficients, i.e., the first-order Taylor expansion of the Fresnel coefficients with respect to the in-plane wave vector:

$$b_p=b_{p\theta_i}+\frac{\partial b_p}{\partial\theta_i}\frac{k_{x_i}}{k_0},\quad b_s=b_{s\theta_i}+\frac{\partial b_s}{\partial\theta_i}\frac{k_{x_i}}{k_0}, \tag{A3}$$

where $b_{p\theta_i}$ and $b_{s\theta_i}$ are the Fresnel coefficients corresponding to the central wave vector, and k_{x_i} is the wave-vector

component along the x_i axis. By incorporating the boundary condition $k_{x_b} = k_{x_i}/\gamma_b$ and Eq. (A3), the matrix $\hat{V}_b$ can be further refined as

$$\hat{W}_b = \begin{bmatrix} b_{p\theta_i} + \gamma_b \frac{\partial b_p}{\partial \theta_i} \frac{k_{x_b}}{k_0} & \frac{k_{y_b}(b_{p\theta_i} - \gamma_b b_{s\theta_i})\cot\theta_i}{k_0} \\ -\frac{k_{y_b}(b_{s\theta_i} - \gamma_b b_{p\theta_i})\cot\theta_i}{k_0} & b_{s\theta_i} + \gamma_b \frac{\partial b_s}{\partial \theta_i} \frac{k_{x_b}}{k_0} \end{bmatrix}, \tag{A4}$$

where we neglect the second-order infinitesimal $k_{x_b}k_{y_b}/k_0^2$. Note that the matrix $\hat{W}_b$ is a Jones matrix defined with horizontal and vertical polarizations as its eigenstates. Next, then, we plan to represent $\hat{W}_b$ as a Jones matrix with LCP and RCP as the eigenstates. The transformation from the linearly polarized basis to the circularly polarized basis can be accomplished through the following matrix:

$$\hat{X} = \frac{1}{\sqrt{2}} \begin{bmatrix} 1 & 1 \\ -i & i \end{bmatrix}. \tag{A5}$$

Finally, the modified Jones matrix in the circularly polarized basis can be expressed as

$$\hat{Y}_b = \hat{X}^{-1}\hat{W}_b\hat{X} = \begin{bmatrix} g1 & g2 \\ g3 & g4 \end{bmatrix}. \tag{A6}$$

Here,

$$g1 = \frac{b_{p\theta_i} + b_{s\theta_i}}{2} - i\frac{k_{y_b}(b_{p\theta_i} + b_{s\theta_i})(1-\gamma_b)\cot\theta_i}{2k_0} + \frac{k_{x_b}\left(\frac{\partial b_p}{\partial \theta_i} + \frac{\partial b_s}{\partial \theta_i}\right)\gamma_b}{2k_0}, \tag{A7a}$$

$$g2 = \frac{b_{p\theta_i} - b_{s\theta_i}}{2} + i\frac{k_{y_b}(b_{p\theta_i} - b_{s\theta_i})(1+\gamma_b)\cot\theta_i}{2k_0} + \frac{k_{x_b}\left(\frac{\partial b_p}{\partial \theta_i} - \frac{\partial b_s}{\partial \theta_i}\right)\gamma_b}{2k_0}, \tag{A7b}$$

$$g3 = \frac{b_{p\theta_i} - b_{s\theta_i}}{2} - i\frac{k_{y_b}(b_{p\theta_i} - b_{s\theta_i})(1+\gamma_b)\cot\theta_i}{2k_0} + \frac{k_{x_b}\left(\frac{\partial b_p}{\partial \theta_i} - \frac{\partial b_s}{\partial \theta_i}\right)\gamma_b}{2k_0}, \tag{A7c}$$

$$g4 = \frac{b_{p\theta_i} + b_{s\theta_i}}{2} + i\frac{k_{y_b}(b_{p\theta_i} + b_{s\theta_i})(1-\gamma_b)\cot\theta_i}{2k_0} + \frac{k_{x_b}\left(\frac{\partial b_p}{\partial \theta_i} + \frac{\partial b_s}{\partial \theta_i}\right)\gamma_b}{2k_0}. \tag{A7d}$$

Based on the relationship between Fresnel coefficients in the linearly polarized basis and the circularly polarized basis, i.e., $b_{++(\theta_i)} = b_{--(\theta_i)} = \frac{b_{p\theta_i}+b_{s\theta_i}}{2}$, $b_{+-(\theta_i)} = b_{-+(\theta_i)} = \frac{b_{p\theta_i}-b_{s\theta_i}}{2}$, $b_{++} = b_{--} = \frac{b_p+b_s}{2}$, and $b_{+-} = b_{-+} = \frac{b_p-b_s}{2}$, $g1$, $g2$, $g3$, and $g4$ can be simplified as

$$\begin{aligned} g1 &= b_{++(\theta_i)} - i\frac{k_{y_b}(1-\gamma_b)\cot\theta_i b_{++(\theta_i)}}{k_0} + \frac{k_{x_b}\frac{\partial b_{++}}{\partial \theta_i}\gamma_b}{k_0} \\ &= b_{++(\theta_i)}\left(1 - ik_{y_b}\delta_{y_{b++}} + k_{x_b}\Delta_{x_{b++}}\right) \\ &= b_{++(\theta_i)}\exp\left(k_{x_b}\Delta_{x_{b++}}\right)\exp\left(-ik_{y_b}\delta_{y_{b++}}\right), \end{aligned} \tag{A8a}$$

$$\begin{aligned} g2 &= b_{+-(\theta_i)} + i\frac{k_{y_b}(1+\gamma_b)\cot\theta_i b_{+-(\theta_i)}}{k_0} + \frac{k_{x_b}\frac{\partial b_{+-}}{\partial \theta_i}\gamma_b}{k_0} \\ &= b_{+-(\theta_i)}\left(1 - ik_{y_b}\delta_{y_{b+-}} + k_{x_b}\Delta_{x_{b+-}}\right) \\ &= b_{+-(\theta_i)}\exp\left(k_{x_b}\Delta_{x_{b+-}}\right)\exp\left(-ik_{y_b}\delta_{y_{b+-}}\right), \end{aligned} \tag{A8b}$$

$$\begin{aligned} g3 &= b_{-+(\theta_i)} - i\frac{k_{y_b}(1+\gamma_b)\cot\theta_i b_{-+(\theta_i)}}{k_0} + \frac{k_{x_b}\frac{\partial b_{-+}}{\partial \theta_i}\gamma_b}{k_0} \\ &= b_{-+(\theta_i)}\left(1 - ik_{y_b}\delta_{y_{b-+}} + k_{x_b}\Delta_{x_{b-+}}\right) \\ &= b_{-+(\theta_i)}\exp\left(k_{x_b}\Delta_{x_{b-+}}\right)\exp\left(-ik_{y_b}\delta_{y_{b-+}}\right), \end{aligned} \tag{A8c}$$

$$\begin{aligned} g4 &= b_{--(\theta_i)} + i\frac{k_{y_b}(1-\gamma_b)\cot\theta_i b_{--(\theta_i)}}{k_0} + \frac{k_{x_b}\frac{\partial b_{--}}{\partial \theta_i}\gamma_b}{k_0} \\ &= b_{--(\theta_i)}\left(1 - ik_{y_b}\delta_{y_{b--}} + k_{x_b}\Delta_{x_{b--}}\right) \\ &= b_{--(\theta_i)}\exp\left(k_{x_b}\Delta_{x_{b--}}\right)\exp\left(-ik_{y_b}\delta_{y_{b--}}\right). \end{aligned} \tag{A8d}$$

Here, $\delta_{y_{b++}} = \cot\theta_i(1-\gamma_b)/k_0$, $\delta_{y_{b-+}} = \cot\theta_i(1+\gamma_b)/k_0$, $\delta_{y_{b+-}} = -\delta_{y_{b-+}}$, $\delta_{y_{b--}} = -\delta_{y_{b++}}$, $\Delta_{x_{b++}} = \gamma_b(\partial \ln b_{++}/\partial\theta_i)/k_0$, $\Delta_{x_{b-+}} = \gamma_b(\partial \ln b_{-+}/\partial\theta_i)/k_0$, $\Delta_{x_{b+-}} = \Delta_{x_{b-+}}$, and $\Delta_{x_{b--}} = \Delta_{x_{b++}}$. We neglect two second-order infinitesimals, $k_{x_b}k_{y_b}/k_0^2$ and $k_{x_b}^2/k_0^2$, and once again apply the first-order approximation condition from the Taylor series expansion, as $k_{y_b}\delta_{y_{b++}}$, $k_{y_b}\delta_{y_{b-+}}$, $k_{y_b}\delta_{y_{b+-}}$, $k_{y_b}\delta_{y_{b--}}$, $k_{x_b}\Delta_{x_{b++}}$, $k_{x_b}\Delta_{x_{b-+}}$, $k_{x_b}\Delta_{x_{b+-}}$, and $k_{x_b}\Delta_{x_{b--}}$ approach zero. By substituting Eqs. (A8a) through (A8d) into Eq. (A6), we then obtain the matrix $\hat{Y}_b$ as given in Eq. (6) in the text.

APPENDIX B: DETAILED EXPRESSIONS OF THE WAVE FUNCTIONS OF THE LCP AND RCP COMPONENTS OF THE SECONDARY FIELD

We consider the incident beam as an arbitrarily polarized vortex beam with the waist located at the interface, and its initial state can be written as follows,

$$|\Psi_i\rangle = \iint dk_{x_i}dk_{y_i}\Phi(k_{x_i}, k_{y_i})|k_{x_i}\rangle|k_{y_i}\rangle|\psi_i\rangle, \tag{B1}$$

where $\iint dk_{x_i}dk_{y_i}\Phi(k_{x_i}, k_{y_i})|k_{x_i}\rangle|k_{y_i}\rangle$ is the momentum representation of incident vortex beams, and $|\psi_i\rangle = C_p[(1+\alpha_c)|+\rangle + (1-\alpha_c)|-\rangle]$ is an arbitrary polarization state. Upon partial reflection and transmission at an interface between two media, the relationship between the incident and secondary fields can be represented as

$$|\Psi_b\rangle = \hat{Y}_b|\Psi_i\rangle = |\Psi_{b+}\rangle + |\Psi_{b-}\rangle. \tag{B2}$$

Here,

$$\begin{aligned} |\Psi_{b+}\rangle &= \iint dk_{x_b}dk_{y_b}\Phi(k_{x_b}, k_{y_b})|k_{x_b}\rangle|k_{y_b}\rangle|+\rangle \\ &\quad \times [C_p(1+\alpha_c)g1 + C_p(1-\alpha_c)g2], \end{aligned} \tag{B3a}$$

$$\begin{aligned} |\Psi_{b-}\rangle &= \iint dk_{x_b}dk_{y_b}\Phi(k_{x_b}, k_{y_b})|k_{x_b}\rangle|k_{y_b}\rangle|-\rangle \\ &\quad \times [C_p(1+\alpha_c)g3 + C_p(1-\alpha_c)g4]. \end{aligned} \tag{B3b}$$

$|\Psi_{b+}\rangle$ and $|\Psi_{b-}\rangle$ are the wave functions of the LCP and RCP components of the secondary field. $\iint dk_{x_b}dk_{y_b}\Phi(k_{x_b}, k_{y_b})|k_{x_b}\rangle|k_{y_b}\rangle$ is the momentum representation of secondary vortex beams. Its relationship with the

incident vortex beam can be determined through the boundary conditions $k_{y_b} = k_{y_i}$ and $k_{x_b} = k_{x_i}/\gamma_b$.

APPENDIX C: ADDITIONAL POLARIZATION-INDEPENDENT ANGULAR SHIFT IN THE x_t DIRECTION

Since the polarization-independent angular shift arises from changes in the cross-sectional geometry of the vortex beam during transmission, and is independent of both in-plane and out-of-plane deflections, we can disregard spin spatial and angular shifts when calculating this polarization-independent angular shift. Equation (B3) can thus be simplified as follows:

$$|\Psi_{t+}\rangle = \iint dk_{x_t} dk_{y_t} \Phi(k_{x_t}, k_{y_t}) |k_{x_t}\rangle |k_{y_t}\rangle |+\rangle \times \left[C_p(1+\alpha_c) t_{++(\theta_i)} + C_p(1-\alpha_c) t_{+-(\theta_i)}\right], \quad \text{(C1a)}$$

$$|\Psi_{t-}\rangle = \iint dk_{x_t} dk_{y_t} \Phi(k_{x_t}, k_{y_t}) |k_{x_t}\rangle |k_{y_t}\rangle |-\rangle \times \left[C_p(1+\alpha_c) t_{-+(\theta_i)} + C_p(1-\alpha_c) t_{--(\theta_i)}\right]. \quad \text{(C1b)}$$

Here, since we only consider transmission, b is represented as t. The total energy density of the transmitted light can then be expressed as

$$\mathbf{Q}_t = n\gamma_t(\langle\Psi_{t+}|\Psi_{t+}\rangle + \langle\Psi_{t-}|\Psi_{t-}\rangle). \quad \text{(C2)}$$

Here, n is the refractive index of the transmitting medium. Since γ_t is closely related to the incident angle θ_i, we perform a Taylor series expansion of γ_t with respect to the in-plane wave vector and retain only the first-order approximation:

$$\gamma_t = \gamma_{t\theta_i} + \frac{\partial\gamma_t}{\partial\theta_i}\frac{k_{x_i}}{k_0} = \gamma_{t\theta_i} + \gamma_t\frac{\partial\gamma_t}{\partial\theta_i}\frac{k_{x_t}}{k_0}. \quad \text{(C3)}$$

Here, $\gamma_{t\theta_i}$ is the coefficient corresponding to central wave vector. The additional in-plane angular shift of the entire transmitted light field can be expressed as

$$\Delta_{x_t}^{add} = \frac{\iint k_{x_t}\mathbf{Q}_t dk_{x_t} dk_{y_t}}{\iint \mathbf{Q}_t dk_{x_t} dk_{y_t}} = (|l|+1)\frac{1}{2R\gamma_t^2}\frac{\partial\gamma_t}{\partial\theta_i}. \quad \text{(C4)}$$

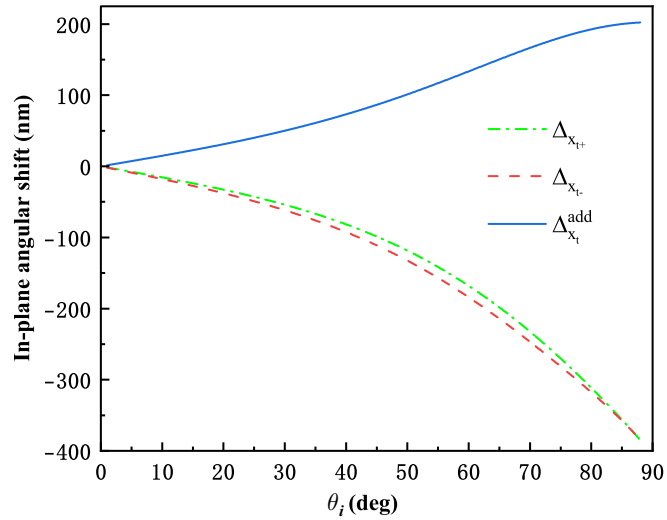


FIG. 4. Variation of in-plane angular shift with incident angle during transmission. The parameters are refractive index of the transmitting medium $n = 1.5$, topological charge $l = 2$, wavelength $\lambda = 632.8$ nm, beam waist $\omega_0 = 27$ μm, $\mathrm{Re}\,\alpha_c = 1$, and $\mathrm{Im}\,\alpha_c = 1$. The angular shift is presented in the form of the spatial shift over the transmission Rayleigh range.

R is the Rayleigh length. It should be noted that this angular shift is independent of α_c, and thus independent of the incident polarization state.

From Eqs. (C3) and (C4), we observe that the polarization-independent angular shift originates from the dispersion relation of the deformation coefficient. It represents the influence of the beam cross-sectional shape change—specifically the stretching and compression of the in-plane wave vector with an unchanged out-of-plane component—on the beam shift. In previous theories, this angular shift may have been overlooked because it is a very small quantity and appears negligible. Few studies consider that the shape deformation of the beam cross section during transmission can also lead to a polarization-independent in-plane angular shift of the entire beam. As shown in Fig. 4, the angular shift is comparable in magnitude to the polarization-dependent in-plane angular shifts ($\Delta_{x_{t+}}$ and $\Delta_{x_{t-}}$), and therefore cannot be neglected.

APPENDIX D: COMPARISON WITH BLIOKH *ET AL.*

A comparison between our work and that of Bliokh *et al.* [34] is presented in Table I.

TABLE I. Comparison with Bliokh *et al.*

Aspect of Comparison	Bliokh *et al.*	Our Work
Wave function treatment	Calculated only the overall wave functions of the reflected and transmitted fields	Extended to include spin-dependent effects (see Appendix B)
Centroid shift	Considered centroid shifts of the overall optical field only	Extended to spin-dependent centroid shifts [see Eqs. (7) and (8)]
Polarization-dependent spatial shifts	Asymmetric expressions in x and y directions due to omission of in-plane spin shifts	Symmetric expressions in x and y directions including spin contributions [see Eqs. (7a)–(7d)]
Polarization-dependent angular shifts	Scaled total angular shift by a factor of $1 + \|m\|$	Extended angular shift relation to spin-dependent form [see Eqs. (8a)–(8d)]

TABLE I. (*Continued*.)

Aspect of Comparison	Bliokh *et al.*	Our Work
Polarization-independent shifts	Only reported polarization-independent spatial shift in y direction	Revealed polarization-independent angular shift in x direction [see Eqs. (12c), (12d), (13a), (13b); see Appendix C]
Linear momentum conservation	Analyzed angular shift without resolving LCP/RCP components	Extended to spin-dependent scenarios, resolving LCP and RCP [see Eq. (14)]
Angular momentum conservation (z-direction)	Used total angular momentum without resolving SAM or OAM for LCP/RCP components	Resolved SAM or OAM for LCP/RCP; extended SAM or OAM to spin-dependent form [see Eq. (15)]
Unified spin-dependent shift structure	Not discussed	Established a unified, symmetric framework for all types of spin-dependent shifts [see Eqs. (9a)–(10d)]

[1] M. Born and E. Wolf, *Principles of Optics: Electromagnetic Theory of Propagation, Interference, and Diffraction of Light* (Elsevier, Oxford, UK, 2013).

[2] F. Goos and H. Hänchen, A new and fundamental experiment on total reflection, Ann. Phys. (NY) **436**, 333 (1947).

[3] C. Imbert, Calculation and experimental proof of the transverse shift induced by total internal reflection of a circularly polarized light beam, Phys. Rev. D **5**, 787 (1972).

[4] F. I. Fedorov, To the theory of total reflection, J. Opt. **15**, 014002 (2013).

[5] K. Y. Bliokh and A. Aiello, Goos–Hänchen and Imbert–Fedorov beam shifts: An overview, J. Opt. **15**, 014001 (2013).

[6] M. Onoda, S. Murakami, and N. Nagaosa, Hall effect of light, Phys. Rev. Lett. **93**, 083901 (2004).

[7] K. Y. Bliokh and Y. P. Bliokh, Conservation of angular momentum, transverse shift, and spin Hall effect in reflection and refraction of an electromagnetic wave packet, Phys. Rev. Lett. **96**, 073903 (2006).

[8] O. Hosten and P. Kwiat, Observation of the spin Hall effect of light via weak measurements, Science **319**, 787 (2008).

[9] K. Y. Bliokh and F. Nori, Transverse and longitudinal angular momenta of light, Phys. Rep. **592**, 1 (2015).

[10] X. Ling, X. Zhou, K. Huang, Y. Liu, C. Qiu, H. Luo, and S. Wen, Recent advances in the spin Hall effect of light, Rep. Prog. Phys. **80**, 066401 (2017).

[11] Y. Qin, Y. Li, X. Feng, Y.-F. Xiao, H. Yang, and Q. Gong, Observation of the in-plane spin separation of light, Opt. Express **19**, 9636 (2011).

[12] X. Qiu, Z. Zhang, L. Xie, J. Qiu, F. Gao, and J. Du, Incident-polarization-sensitive and large in-plane-photonic-spin-splitting at the Brewster angle, Opt. Lett. **40**, 1018 (2015).

[13] W. Zhen, X.-L. Wang, J. Ding, and H.-T. Wang, Revisiting physical mechanism of longitudinal photonic spin splitting and Goos-Hänchen shift, New J. Phys. **26**, 013045 (2024).

[14] Y. Gorodetski, K. Y, Bliokh, B. Stein, C. Genet, N. Shitrit, V. Kleiner, E. Hasman, and T. W. Ebbesen, Weak measurements of light chirality with a plasmonic slit, Phys. Rev. Lett. **109**, 013901 (2012).

[15] N. Shitrit, I. Yulevich, E. Maguid, D. Ozeri, D. Veksler, V. Kleiner, and E. Hasman, Spin-optical metamaterial route to spin-controlled photonics, Science **340**, 724 (2013).

[16] K. Y. Bliokh, D. Smirnova, and F. Nori, Quantum spin Hall effect of light, Science **348**, 1448 (2015).

[17] X. Zhou and X. Ling, Enhanced photonic spin Hall effect due to surface plasmon resonance, IEEE Photonics J. **8**, 4801108 (2016).

[18] X. Yin, Z. Ye, J. Rho, Y. Wang, and X. Zhang, Photonic spin Hall effect at metasurfaces, Science **339**, 1405 (2013).

[19] W. Luo, S. Xiao, Q. He, S. Sun, and L. Zhou, Photonic spin Hall effect with nearly 100% efficiency, Adv. Opt. Mater. **3**, 1102 (2015).

[20] B. Wang, K. Rong, E. Maguid, V. Kleiner, and E. Hasman, Probing nanoscale fluctuation of ferromagnetic meta-atoms with a stochastic photonic spin Hall effect, Nat. Nanotechnol. **15**, 450 (2020).

[21] T. Zhu, Y. Lou, Y. Zhou, J. Zhang, J. Huang, Y. Li, H. Luo, S. Wen, S. Zhu, Q. Gong, M. Qiu, and Z. Ruan, Generalized spatial differentiation from the spin Hall effect of light and its application in image processing of edge detection, Phys. Rev. Appl. **11**, 034043 (2019).

[22] R. Wang, S. He, and H. Luo, Photonic spin-Hall differential microscopy, Phys. Rev. Appl. **18**, 044016 (2022).

[23] W. J. M. Kort-Kamp, Topological phase transitions in the photonic spin Hall effect, Phys. Rev. Lett. **119**, 147401 (2017).

[24] S. Chen, X. Ling, W. Shu, H. Luo, and S. Wen, Precision measurement of the optical conductivity of atomically thin crystals via the photonic spin Hall effect, Phys. Rev. Appl. **13**, 014057 (2020).

[25] W. Zhang, Y. Wang, S. Chen, S. Wen, and H. Luo, Photonic spin Hall effect in twisted few-layer anisotropic two-dimensional atomic crystals, Phys. Rev. A **105**, 043507 (2022).

[26] M. Shah, M. S. Anwar, R. Asgari, and G. Xianlong, Photonic spin Hall effect in Haldane model materials, Phys. Rev. B **109**, 235418 (2024).

[27] J. Wang, L. Shi, and J. Zi, Spin Hall effect of light via momentum-space topological vortices around bound states in the continuum, Phys. Rev. Lett. **129**, 236101 (2022).

[28] F. Wu, T. Liu, Y. Long, S. Xiao, and G. Chen, Giant photonic spin Hall effect empowered by polarization-dependent quasi-bound states in the continuum in compound grating waveguide structures, Phys. Rev. B **107**, 165428 (2023).

[29] G. Wan, Z. Ma, Y. Xue, C. Zhang, Y. Chen, and X. Zhou, Photonic spin Hall effect at an optical bound state in the continuum, Phys. Rev. B **111**, 085411 (2025).

[30] X. Ling, F. Guan, Z. Zhang, H.-X. Xu, S. Xiao, and H. Luo, Vortex mode decomposition of the topology-induced phase transitions in spin-orbit optics, Phys. Rev. A **104**, 053504 (2021).

[31] W. Zhen, X.-L. Wang, J. Ding, and H.-T. Wang, Controlling the symmetry of the photonic spin Hall effect by an optical vortex pair, Phys. Rev. A **108**, 023514 (2023).

[32] L. Allen, M. W. Beijersbergen, R. J. C. Spreeuw, and J. P. Woerdman, Orbital angular momentum of light and the transformation of Laguerre-Gaussian laser modes, Phys. Rev. A **45**, 8185 (1992).

[33] Y. Shen, X. Wang, Z. Xie, C. Min, X. Fu, Q. Liu, M. Gong, and X. Yuan, Optical vortices 30 years on: OAM manipulation from topological charge to multiple singularities, Light Sci. Appl. **8**, 90 (2019).

[34] K. Y. Bliokh, I. V. Shadrivov, and Y. S. Kivshar, Goos–Hänchen and Imbert–Fedorov shifts of polarized vortex beams, Opt. Lett. **34**, 389 (2009).

[35] H. Luo, X. Ling, X. Zhou, W. Shu, S. Wen, and D. Fan, Enhancing or suppressing the spin Hall effect of light in layered nanostructures, Phys. Rev. A **84**, 033801 (2011).

[36] X. Ling, W. Xiao, S. Chen, X. Zhou, H. Luo, and L. Zhou, Revisiting the anomalous spin-Hall effect of light near the Brewster angle, Phys. Rev. A **103**, 033515 (2021).

[37] L. Xie, J. Zhu, G. Ren, F. Yang, L. Xu, Y. Dan, and Z. Zhang, Particle nature of the photonic spin Hall effect, Opt. Express **32**, 9468 (2024).

[38] D. Stoler, Operator methods in physical optics, J. Opt. Soc. Am. **71**, 334 (1981).

[39] A. Aiello, N. Lindlein, C. Marquardt, and G. Leuchs, Transverse angular momentum and geometric spin Hall effect of light, Phys. Rev. Lett. **103**, 100401 (2009).

[40] K. Y. Bliokh, M. A. Alonso, E. A. Ostrovskaya, and A. Aiello, Angular momenta and spin-orbit interaction of nonparaxial light in free space, Phys. Rev. A **82**, 063825 (2010).

[41] K. Y. Bliokh, F. J. Rodríguez-Fortuño, F. Nori, and A. V. Zayats, Spin-orbit interactions of light, Nat. Photon. **9**, 796 (2015).